Journal of Hepatocellular Carcinoma

Dovepress
Taylor & Francis Group

Open Access Full Text Article

ORIGINAL RESEARCH

Construction of a Prognostic Model Based on Insulin Resistance-Related Genes to Predict TACE Response and Identification of PD-98059 as a Potential Therapeutic Agent

Weitao Wang*, Kang Chen*, Chen Fan, Lei Sun, Haohuan Tang, Wei Ding, Feihu Sun, Weidong Wang

Department of Interventional Radiology, The Affiliated Wuxi People's Hospital of Nanjing Medical University, Wuxi, People's Republic of China

*These authors contributed equally to this work

Correspondence: Feihu Sun; Weidong Wang, Email 907822062@qq.com; Wdoc@sina.com

Purpose: Transarterial chemoembolization (TACE) is the primary treatment for unresectable hepatocellular carcinoma (HCC). Given the poor prognosis of liver cancer patients with diabetes, identifying indicators of response to TACE and methods to reverse non-response is crucial.

Methods: Patients were classified as TACE-responsive or non-responsive in the GSE104580 dataset. We conducted Kyoto Encyclopedia of Genes and Genomes (KEGG) analysis to identify the differentially expressed genes (DEGs). Univariate and multivariate Cox regression analyses were performed on genes in the insulin resistance signaling pathway to screen for those associated with poor prognosis in TACE. We developed a polygenic signature in GSE14520 using LASSO Cox regression, conducted molecular docking of four genes with drugs, and validated the results using drug sensitivity tests. The Connectivity Map (CMap) database was used to identify potential drugs for reversing TACE.

Results: We constructed a prognostic signature consisting of four genes (DUSP9, ENO2, NTS, and SERPINE1) and validated it using drug-sensitivity tests. Classifying TACE-treated patients into high- and low-risk groups using risk scores revealed that the high-risk group had significantly lower overall survival than the low-risk group. In patients undergoing TACE, the risk score independently predicted overall survival. Using the CMap database, we speculated that PD-98059 is a potential drug for reversing TACE unresponsiveness. We detected the docking sites of PD-98059 in four genes. Cell experiments confirmed that PD-98059 synergistically enhanced the inhibitory effect of lobaplatin on HCC cell proliferation.

Conclusion: The insulin resistance model tailored for TACE effectively predicts patient prognosis. Via the effect of MEK inhibitor PD-98059, the efficacy of TACE in patients can be improved.

Keywords: TACE, insulin resistance, prognosis, hepatocellular carcinoma, molecular docking, chemotherapy

Introduction

Hepatocellular carcinoma (HCC) is a prevalent form of liver cancer, with over 700,000 new cases diagnosed globally each year, half of which occur in China.[1] The primary treatment options for liver cancer include surgery, interventional therapy, radiotherapy, chemotherapy, and palliative care, with surgery being the preferred approach for early-stage patients.[2] Transcatheter arterial chemoembolization (TACE) involves the administration of antitumor drugs into the artery supplying the liver tumor. It is mainly used for locally advanced HCC, which is unsuitable for surgical resection or liver transplantation.[3] The Barcelona Clinic Liver Cancer (BCLC) staging system recommends TACE as the first-line treatment for intermediate-stage (BCLC B) patients.[4] Nonetheless, TACE may lose effectiveness over repeated applications, a phenomenon termed TACE refractoriness or TACE failure by the Japanese Society of Liver Diseases in 2010.[5]

https://doi.org/10.2147/JHC.S553710
Received: 14 July 2025
Accepted: 3 January 2026
Published: 21 January 2026

TACE refractoriness is characterized by an unsatisfactory tumor response or rapid disease progression, which inevitably leads to poor survival outcomes. Therefore, it is imperative to elucidate the molecular drivers of TACE resistance and establish a robust prognostic model to identify high-risk patients in advance.

In addition to its established role in metabolism, insulin resistance (IR) is associated with poor prognosis in various cancers, including HCC.[6,7] Research has demonstrated a clear association between diabetes and cancer. Patients with both liver cancer and type 2 diabetes had faster growing tumors and worse outlooks than those who only had liver cancer.[8] IR is a crucial link between diabetes and liver cancer risk factors such as viral hepatitis, fatty liver disease, and cirrhosis.[9,10] IR denotes the diminished effect of insulin on target organs. Reduced insulin sensitivity or function hinders glucose metabolism, leading to elevated blood glucose levels and creating a tumor-promoting microenvironment. IR disrupts glucose metabolism in hepatocytes, with elevated blood glucose levels fueling tumor cell growth.[10] More importantly, the presence of diabetes can negatively impact the long-term survival of patients with mid-stage HCC undergoing TACE, including reduced treatment response rates and shorter time to progression.[11] Therefore, investigating the link between IR and TACE resistance is crucial to enhance the prognosis of patients with liver cancer treated with TACE.

Preoperative screening for patients who are likely to benefit from TACE has garnered interest.[12] Several prognostic models have been proposed, including the hepatocellular artery embolization prognosis (HAP) score and its subsequent improvements such as mHAP, mHAP II, and mHAP III. These models integrate serum biomarkers, tumor burden, and radiological features to predict TACE response.[13,14] Although these models are easy to apply in clinical settings and show practicality in stratifying patient risks, they still have limitations. First, they mostly rely on traditional clinical indicators and may not fully capture the molecular heterogeneity of HCC. Second, although they provide aggregated risk estimates, they cannot update the prognosis with the disease process as some emerging dynamic prediction models (For example, Shen et al established and compared two dynamic prognostic prediction models, "survival path" and "Dynamic-DeepHit", based on time series data from large cohorts), and the biological contribution of individual factors to TACE refractory or failure is not clear.[15] As a total score, specific molecular pathways that control treatment susceptibility or drug resistance, such as molecular pathways associated with IR, are not well revealed. According to Feng et al, model development is necessary at this time.[16] Constructing a predictive model based on insulin resistance-related genes is a reasonable strategy to overcome these limitations because it directly detects the biology of TACE response and has the potential to improve prognostic accuracy while identifying new therapeutic targets.

In this research, the GEO dataset was utilized to build a prognostic signature made up of four genes-DUSP9, ENO2, NTS, and SERPINE1 for predicting the outcomes of TACE, cell lines were divided into TACE - responsive and TACE-non-responsive groups according to insulin - resistant gene expression profiles and then comparative analyses were carried out to confirm the effectiveness of these profiles, by using the CMAP database, the MEK inhibitor PD-98059 was found and it was shown that it could increase the sensitivity of hepatoma cells to a TACE - like treatment in vitro, the initial exploration of a new TACE therapeutic regimen in this study, whether during or after surgery, emphasizes the necessity for future randomized clinical trials to verify these results. This study provides a new supplement to the prognosis of HCC patients receiving TACE and provides a new treatment strategy for doctors to treat and predict the prognosis of HCC patients.

Materials and Methods

Data Sources

In the GSE104580 cohort dataset, 147 patients with HCC who received TACE treatment were included. Of these, 81 patients responded well to TACE (TACE-responsive), whereas 66 did not (TACE-non-responsive). The TACE treatment subgroup (n = 104) was extracted from GSE14520 as an external validation cohort-GSE14520-TACE subgroup.[17,18] The 104 patients in GSE14520 included 74 patients with HCC who underwent TACE after hepatectomy and 30 patients with recurrent HCC who were treated with TACE. Cox regression and Kaplan-Meier survival analyses were performed. This study also integrated transcriptome data from The Cancer Genome Atlas (TCGA)-LIHC and Genotype-Tissue Expression (GTEx) databases and included protein expression profiles of normal and hepatocellular carcinoma tissues

in the Human Protein Atlas (HPA) database. Information about the patients' response to treatment in the two datasets was provided by the original author.

Establishment of Gene Signatures Associated with Potential Prognostic Insulin Resistance Signaling Pathways

Utilizing the R-based limma package, we identified differentially expressed genes (DEGs) in the GSE104580 dataset between TACE-responsive and TACE-non-responsive groups. The criteria for DEGs included a false discovery rate (FDR) below 0.05, an absolute $\log_2$ fold change (|log2FC|) exceeding 1.5, and a p-value < 0.05. Following the differential expression study, KEGG (Kyoto Encyclopedia of Genes and Genomes) pathway analysis was performed on the altered genes in the TACE-non-responsive group using the cluster Profiler R package. Fourteen genes associated with the insulin resistance signaling pathway were identified and subjected to univariate and multivariate regression analyses in the GSE14520-TACE subgroup dataset, revealing genes linked to survival. In order to make predictive features more precise and help with subset reduction, LASSO regression was done with the glmnet package in R, finally resulting in the obtaining of a risk score calculation formula: $Riskscore = \sum_{i=1}^{n}[expression\ of\ Genei \times \beta i]$, Let n represent the overall number of genes existing in the signature and let β stand for the regression coefficient obtained for these genes through the LASSO regression analysis. Kaplan-Meier and time-dependent receiver operating characteristic (ROC) curves were used to evaluate the performance of the model.

Detection of Potential Compounds

Utilizing the Connectivity Map (CMap) database (https://clue.io/CMap), which identifies potential drugs by matching gene expression profiles of cell lines to various drugs, we input the significantly upregulated genes from the GSE14520-TACE subgroup medium- and high-risk groups into the L1000 platform to identify compounds that might induce reversal responses.[19] Subsequently, we selected a compound with a connectivity score of less than −98 for subsequent cell experiments.

Molecular Docking

Molecular docking was used to verify the binding activity between the active ingredients and key targets. AutoDock Vina (version 1.1.2) employs a semi-flexible docking approach, achieving a docking accuracy of 78%. The crystal structures of DUSP9 (PDB ID: 2hxp), ENO2 (PDB ID: 1te6), NTS (PDB ID: 2lne), and SERPINE1 (PDB ID: 1a7c) were retrieved from the RCSB Protein Data Bank (https://www.pdb.org/), and the structure of PD-98059 was sourced from the PubChem database (https://pubchem.ncbi.nlm.nih.gov/). PyMOL (version 4.3.0) software was used to separate the original ligands and protein structures and for the dehydration and removal of organics. AutoDocktools were used for hydrogenating, checking the charge, specifying the atomic type (Ad4 type), calculating Gasteiger, and constructing the docking grid box of the protein structure. Furthermore, the chemical composition of the small-molecule ligand should be identified at the root, and the ligand torsion bond should be selected using AutoDocktools. In AutoDocktools, the protein structure and small molecule ligand are converted from "Pdb" to "Pdbqt" format for docking. After docking with Vina, protein molecule combination scores were computed, followed by analysis and visualization using the PLIP online platform and LigPlot software.

Cell Culture

Human normal hepatocytes THLE-2, hepatoma cells Huh-7, HepG2, Hep 3 B, SNU-387, and SK-Hep-1 were purchased from the American Type Culture Collection (ATCC, Manassas, VA, USA). Among them, Hep3B is p53-deficient, HepG2 is wild-type p53, and retains many hepatocyte-like metabolic functions.[20,21] Simultaneously, they were derived from HBV-related HCC.[22] Huh-7 and SNU-387 were derived from non-viral HCC, which can more widely represent the origin of the disease.[23,24] SK-Hep-1 is usually described as a highly invasive and metastatic cell line, while Hep3B and HepG2 are considered to be less invasive.[25] Based on the expression patterns of these four molecules, the cell lines were categorized into reactive and nonreactive groups. Huh-7, HepG2, and Hep 3B cell lines were cultured in Dulbecco's modified Eagle's

medium (DMEM) from Life Technologies (Carlsbad, CA, USA), supplemented with 10% fetal bovine serum (FBS, Sigma, St. Louis, Missouri, USA) and 1% penicillin-streptomycin. THLE-2 cells were cultured in BEGM containing 10% FBS and 5 ng/mL EGF. SK-Hep-1 cells were maintained in Minimal Essential Medium (MEM; Life Technologies) enriched with 10% FBS, penicillin, streptomycin, L-glutamine, non-essential amino acids, and sodium pyruvate. SNU-387 cells were grown in RPMI-1640 medium (Life Technologies) supplemented with 10% FBS, penicillin, and streptomycin.

Quantitative Real-Time Polymerase Chain Reaction (qRT-PCR)

We used qRT-PCR to determine the expression of characteristic genes in the cells. Total RNA was extracted from the cells using TRIzol Reagent (Life Technologies) according to the manufacturer's instructions. Subsequently, reverse transcription was performed using the HiScript II Q Select RT SuperMix (Vazyme, Nanjing, Jiangsu, China). Finally, RT-qPCR was performed using SYBR Select Master Mix (Applied Biosystems, South San Francisco, CA, USA) and an ABI7300 system (Applied Biosystems). Relative gene expression levels were calculated using the $2^{-\Delta\Delta Ct}$ method, and GAPDH was used as an internal reference. The primer sequences are as follows: DUSP9: 5 -CAGCCGTTCTGTCACCGTC-3′, 5′-CAAGCTGCGCTCAAAGTCC-3′;ENO2: 5′-AGCCTCTACGGGCATCTATGA-3′, 5′-TTCTCAGTCCCATCCAACTCC-3′; NTS: 5′-AGAGAGAGCCCCCTTCAGTG-3′, 5′-TTCCTCTTCTGAATCTGAGCAC-3′; SERPINE1: 5′-GGTGCTGGTGAATGCCCTCTAC-3′, 5′-TGCTGCCGTCTGATTTGTGGAA-3′;GAPDH: 5′-CCATGGAGAAGGCTGGGG-3′, 5′-CAAAGTTGTCATGGATGACC-3′.

Cell Viability and Drug Sensitivity Analysis

We added 5000 cells per well to a 96-well plate and diluted it with the corresponding cell culture medium. The cells were cultured for 24 h at 37°C in a 5% CO_2 incubator. Subsequently, varying concentrations of lobaplatin (0–64 μg/mL) or PD-98059 (0–512 μM) were administered for 48 hours. Next, 10 μL of WST-8 was added to each well and the cells were incubated for an additional 2 h. Optical density at 450 nm was measured using enzyme calibration (Thermo Fisher, Waltham, MA, USA).

Cell Proliferation Assay

We added 5000 cells per well to a 96-well plate and diluted it with the corresponding cell culture medium; each group had eight replicate wells. The cells were precultured at 37°C and 5% CO_2 for 24 h. Subsequently, the medium was replaced with a drug-containing medium, and lobaplatin, PD-98059, or a combination of the two at the previously determined IC50 concentrations was added. An independent experimental hole was set up for each time point (0,6,12,24,48 hours), and independent experimental hole was set up. After reaching the specified time, 10 μL of WST-8 solution was added to the corresponding well, and the incubation was continued in the incubator for 2 h. The optical density at 450 nm was measured using an enzyme-linked immunosorbent assay (MULTISKAN FC, Thermo Fisher).

Statistical Analysis

Statistical analyses were performed using GraphPad Prism (version 8.0.2) and R software (version 4.3.1). The Kaplan-Meier method was used for survival analysis, and the Log rank test was used to compare differences between groups. An independent sample *t*-test was used to compare continuous variables between groups. One-way ANOVA was used for comparisons between multiple groups. Statistical significance was defined as a two-tailed $P < 0.05$.

Results

The Insulin Resistance Signaling Pathway is Enriched in the TACE-Non-Responsive Group

Analysis of the GSE104580 dataset, comparing gene expression profiles of 81 TACE non-responders and 66 responders, revealed distinct gene regulation patterns. Specifically, 735 genes were more active in the non-responsive group and 749 genes were more active in the responsive group, identified using a log2-fold change threshold greater than 0.5 and a p-value less than

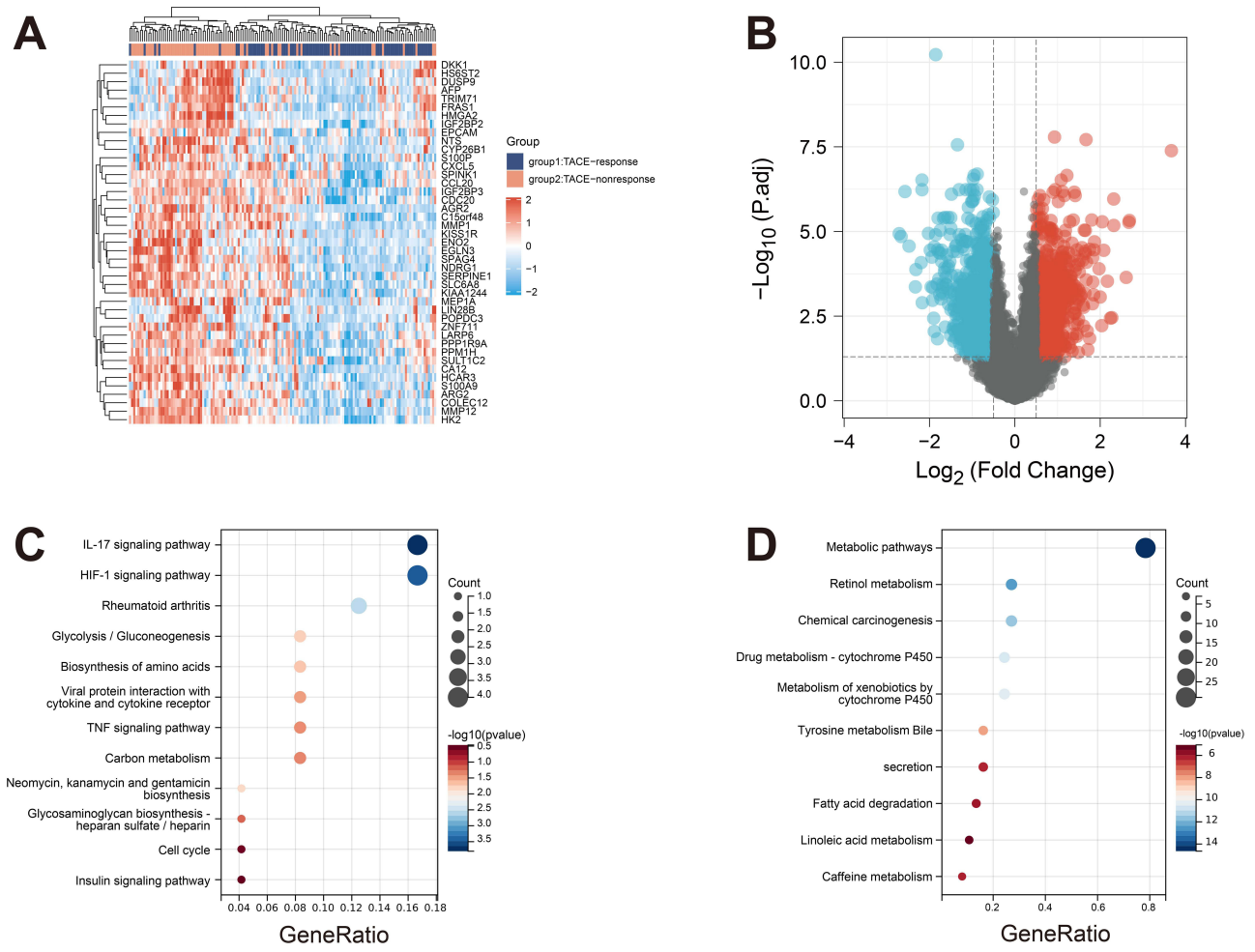

Figure 1 Differences in transcriptome samples between TACE-responsive and TACE-non-responsive groups in GSE104580. (**A**) Heatmap showed the distribution of differentially expressed genes between TACE responders and non-responders. (**B**) Volcano plot showing up-regulated genes in TACE-responsive and TACE-non-responsive groups. (**C** and **D**) Bubble plots showing the enriched KEGG pathway in the TACE non-responsive group and the TACE-responsive group.
Abbreviations: TACE, Transarterial chemoembolization; KEGG, Kyoto Encyclopedia of Genes and Genomes.

0.05 for statistical significance. Next, we created a heatmap (Figure 1A) and a volcano plot (Figure 1B) to visually show these gene expression differences, and then carried out further research through KEGG enrichment analysis, which showed that the insulin signaling pathway was highly enriched in the TACE non - responsive group (Figure 1C), but not in the TACE responsive group (Figure 1D).

Identification of Genes Related to the Insulin Resistance Signaling Pathway That are Associated with TACE Prognosis in GSE14520-TACE Subgroup

We conducted an intersection analysis of insulin resistance-associated genes from the NCBI database and those upregulated in the TACE-non-responsive group, identifying 14 genes enriched in the insulin resistance signaling pathway: AFP, ARG2, CXCL5, DUSP9, EGLN3, ENO2, HK2, IGF2BP2, MMP1, MMP12, NTS, S100A9, SERPINE1, and LIN28B (Figure 2A). Univariate regression analysis on the GSE14520-TACE subgroup dataset assessed the prognostic significance of these genes in TACE-treated patients, revealing that 11 genes were associated with poor prognosis (Table 1). The relationships among these 11 molecular markers are shown in Figure 2B.

https://doi.org/10.2147/JHC.S553710

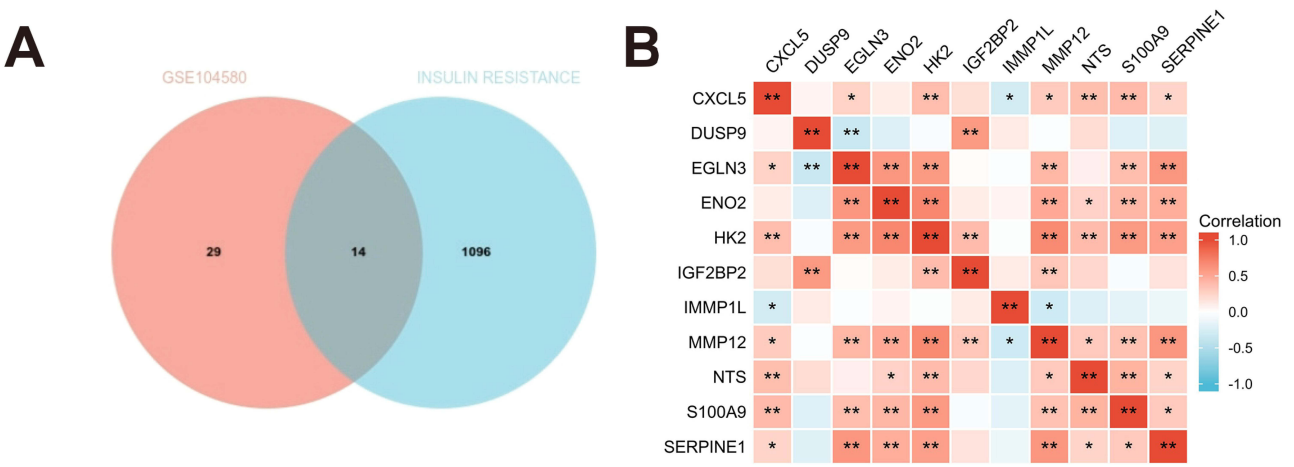

Figure 2 14 IR-related genes and their associations associated with overall survival (OS) in GSE14520-TACE subgroup. (**A**) Venn diagram showing that 14 genes overlapped in the GSE104580 differential gene as well as the insulin resistance pathway. (**B**) The heat map showed the correlation of these genes in the TACE non-response group in the GSE104580 dataset. *P<0.05, **P<0.01.
Abbreviations: OS, overall survival; TACE, Transarterial chemoembolization.

Construction of Prognostic Features

Subsequently, LASSO regression analysis was used to delete redundant IR-related genes from the 11 gene sets for further screening (Figure 3A and B). Finally, four IR-related genes involved in modeling were identified: DUSP9, ENO2, NTS, and SERPINE1. A risk score was calculated for each patient for prognostic evaluation, based on the coefficient and expression level of each IR-related gene. The risk score, calculated as (DUSP9 × 0.19440349) + (ENO2 × 0.05395551) + (NTS × 0.10267704) + (SERPINE1 × 0.26740617), was used to classify the patients into high-risk (n = 52) and low-risk (n = 52) groups based on the median value (Figure 3C). Kaplan-Meier analysis revealed a significantly poorer prognosis for the high-risk group than for the low-risk group (Figure 3D, P < 0.001). The prognostic ability of the model was evaluated by ROC curve. The AUC values at 1-year, 3-year and 5-year were 0.809, 0.8374, and 0.669, respectively (Figure 3E). These results indicate that our model based on these four IR-related genes has better prognostic performance. Furthermore, based on the GSE104580 dataset, the differences in risk core values between TACE non-responders

Table 1 Eleven of the 14 Genes Were Associated with Low OS in TACE-Treated Patients

Characteristics	Total (N)	Univariate Analysis		Multivariate Analysis	
		Hazard Ratio (95% CI)	P value	Hazard Ratio (95% CI)	P value
AFP	104	1.723 (0.947–3.137)	0.075	1.102 (0.571–2.129)	0.772
AGR2	104	1.085 (0.262–4.502)	0.910		
CXCL5	104	2.423 (1.301–4.511)	**0.005**	1.203 (0.622–2.326)	0.583
DUSP9	104	2.555 (1.399–4.665)	**0.002**	2.504 (1.215–5.158)	**0.013**
EGLN3	104	3.629 (1.971–6.679)	**<0.001**	2.055 (0.914–4.619)	0.081
ENO2	104	2.595 (1.396–4.826)	**0.003**	0.882 (0.396–1.967)	0.759
HK2	104	2.423 (1.242–4.727)	**0.009**	0.759 (0.307–1.877)	0.551
IGF2BP2	104	2.056 (1.012–4.175)	**0.046**	1.068 (0.453–2.519)	0.880
MMP1	104	4.262 (1.794–10.129)	**0.001**	2.438 (0.956–6.216)	0.062
MMP12	104	3.720 (1.651–8.382)	**0.002**	1.662 (0.596–4.635)	0.332
NTS	104	3.491 (1.896–6.427)	**<0.001**	1.833 (0.917–3.661)	0.086
S100A9	104	2.044 (1.065–3.920)	**0.032**	1.182 (0.545–2.564)	0.672
SERPINE1	104	3.577 (1.913–6.686)	**<0.001**	2.160 (1.042–4.477)	**0.038**

Notes: Red, showing genes significantly associated with OS in TACE patients in univariate analysis; Bold font, showing p values of less than 0.05. In the univariate analysis, the corresponding genes were associated with OS in patients. In multivariate analysis, the corresponding gene can be used as an independent factor to predict the OS of TACE patients.

https://doi.org/10.2147/JHC.S553710

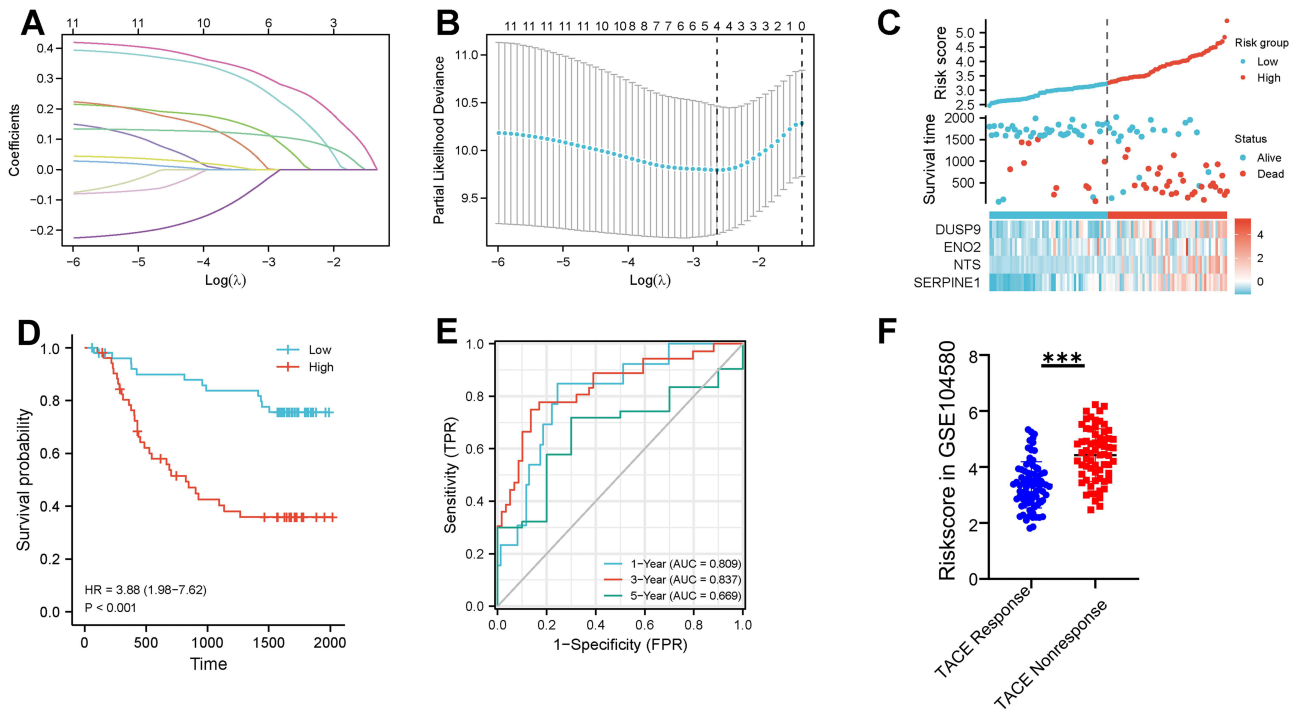

Figure 3 Construction of prognostic features. (**A**) Coefficient profiles generated from logarithmic sequences. (**B**) Lasso coefficient distributions for these 11 genes. (**C**) Risk scores and survival state of patients treated with TACE in GSE14520-TACE subgroup. (**D**) Kaplan–Meier curves show that among patients treated with TACE in GSE14520-TACE subgroup, OS was lower in the high-risk group than in the low-risk group. (**E**) AUC values of the receiver operating characteristic curve (ROC) showing the predicted performance of the prognostic model in GSE14520-TACE subgroup. (**F**) Differences in risk scores between TACE-responsive and TACE-non-responsive groups in GSE104580. ***P<0.001.

Abbreviations: TACE, Transarterial chemoembolization; OS, overall survival; AUC, Area Under the Curve; ROC, receiver operating characteristic.

and responders were analyzed. The results showed that the risk score of TACE non-responders was significantly higher ($P < 0.0001$, Figure 3F).

Predictive Effects of Validation Signatures in Different Clinical Subgroups

The discriminative power of insulin resistance was assessed in patients who underwent TACE by stratifying them into clinical subgroups based on factors such as alpha-fetoprotein (AFP) levels (≤300 ng/mL vs >300 ng/mL), tumor size (≤5 cm vs >5 cm), age (≤50 years vs >50 years), alanine aminotransferase (ALT) levels (≤300 ng/mL vs >300 ng/mL), presence of distant metastases, Barcelona Clinic Liver Cancer (BCLC) stage A, cirrhosis, multinodular (multinodular vs non-multinodular), and TNM stages I, II, and III. Kaplan-Meier curves were used to analyze overall survival (OS) within each group, revealing statistically significant differences that demonstrated a prognostic model based on IR-related genes with strong discriminative ability (Figure 4A–O).

Prognostic Significance of the Signal as an Independent Factor

In order to explore the predictive effect of insulin resistance, we carried out a comparative study of risk scores among diverse clinical groups within the dataset GSE14520-TACE subgroup, which showed that people who had a relapse within 24 months had higher risk scores than those whose relapse occurred after 24 months, which is shown in Figure 5A and supports our clinical results. The risk scores of TNM II and III were significantly higher (Figure 5B), suggesting that insulin resistance could be a useful discriminative biomarker for distinguishing hepatocellular carcinomas (HCCs) according to their TNM grade and might be a good marker for diagnosing liver cancer. Moreover, Figure 5C illustrates that patients with AFP≤300 ng/mL had higher risk scores than those with AFP>300 ng/mL, suggesting that the latter group may experience better outcomes with TACE treatment.

https://doi.org/10.2147/JHC.S553710

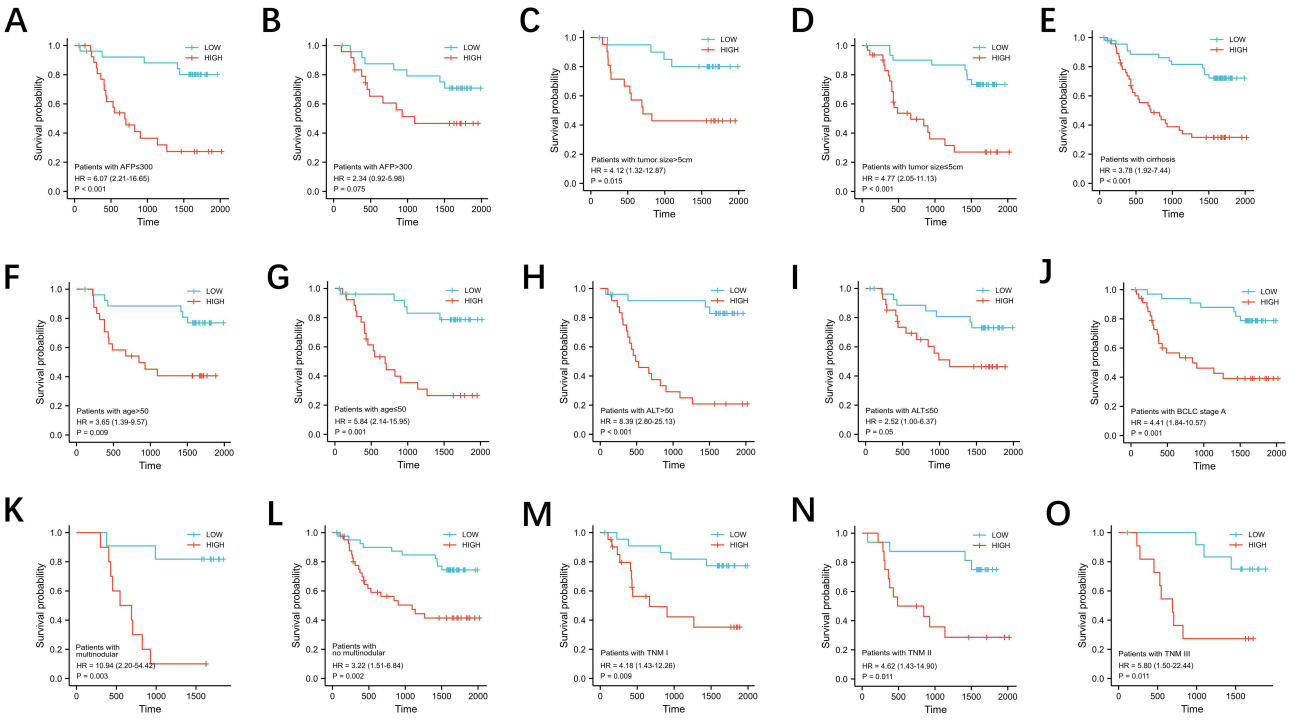

Figure 4 To validate the feature recognition ability of different clinical subgroups in GSE14520-TACE subgroup. (**A-O**) Kaplan-Meier curves was used to analyze the OS difference of patients in different clinical subgroups treated with TACE (AFP ≤ 300 ng/mL and > 300 ng/mL; tumor size ≤ 5 cm and >5 cm; age ≤ 50 and > 50; ALT ≤ 300 ng/mL and > 300 ng/mL; distant metastasis, BCLC stage A; cirrhosis; multinodular; TNM stages I, II and III).
Abbreviations: TACE, Transarterial chemoembolization; OS, overall survival; AFP, alpha-fetoprotein; BCLC, Barcelona Clinic Liver Cancer; TNM, Tumor Node Metastasis.

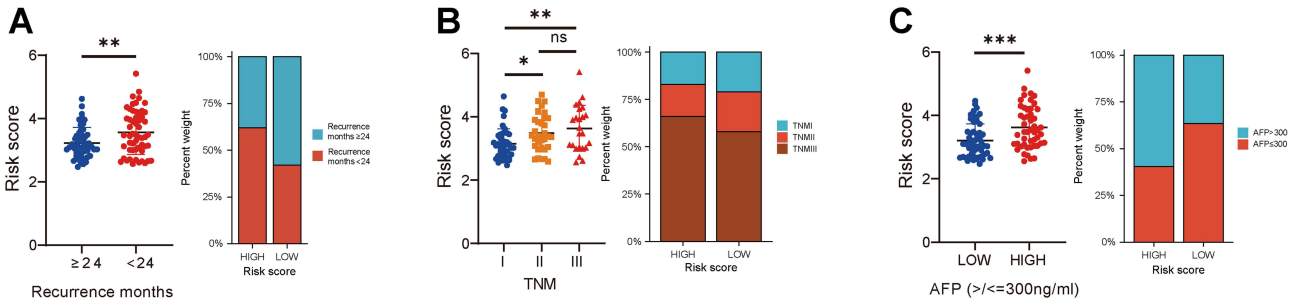

Figure 5 Risk score differences in different clinical subgroups of patients treated with TACE. (**A**) The risk score showed an upward trend with decreasing months of recurrence, (**B**) TNM stage, and (**C**) AFP. *P<0.05, **P<0.01, ***P<0.001. ns, indicates no statistical significance.
Abbreviations: TACE, Transarterial chemoembolization; TNM, Tumor Node Metastasis; AFP, alpha-fetoprotein.

Based on the GSE14520-TACE subgroup data set, univariate Cox regression analysis found that main tumor size (≤ 5 cm, >5 cm), advanced TNM staging (I–II, III), BCLC staging (0 And A, B And C), recurrence months (≤ 24months, >24months), and Riskscore were associated with the overall survival rate of HCC patients treated with TACE (Table 2). Subsequent multivariate Cox regression confirmed that the risk score was an independent predictor (hazard ratio [HR] = 2.109, P < 0.001). 95% confidence interval (CI): 1.287–3.455. These results suggest that the risk core can be used as an independent prognostic factor for patients with HCC treated with TACE.

Expression and Prognostic Profile of the Four Genes

We conducted a comparative analysis of the expression profiles of DUSP9, ENO2, NTS, and SERPINE1 in various normal and tumor tissues using the TCGA and GTEx databases, which included both paired and unpaired samples. Our

Table 2 Univariate and Multivariate Analysis of Overall Survival for GSE14520

Factors	Univariate Analysis		Multivariate Analysis	
	Hazard Ratio (95% CI)	P value	Hazard Ratio (95% CI)	P value
Age (<=50, >50)	1.068 (0.586–1.944)	0.831		
Main Tumor Size (<=5 cm, >5 cm)	1.878 (1.031–3.421)	**0.040**	1.664 (0.582–4.755)	0.342
Multinodular (YSE, NO)	1.172 (0.578–2.380)	0.660		
Cirrhosis (YSE, NO)	7.149 (0.983–51.988)	0.052	10.395 (0.669–161.544)	0.094
TNM staging (I–II, III)	2.923 (1.539–5.551)	**0.001**	1.212 (0.336–4.369)	0.769
BCLC staging (0 And A, B And C)	2.756 (1.454–5.224)	**0.002**	0.871 (0.297–2.549)	0.801
AFP (>300 ng/mL, <=300ng/mL)	0.721 (0.396–1.313)	0.285		
Recurr months (<=24months, >24months)	0.124 (0.057–0.271)	**<0.001**	0.113 (0.046–0.276)	**<0.001**
Riskscore	3.732 (2.415–5.769)	**<0.001**	2.109 (1.287–3.455)	**0.003**

Notes: Bold font, showing p values of less than 0.05. In the univariate analysis, the corresponding genes were associated with OS in patients. In multivariate analysis, the corresponding gene can be used as an independent factor to predict the OS of TACE patients.

study showed that these genes are significantly differentially expressed in most cancers, such as liver and breast cancer (Supplementary Figure 1A–D). Analysis based on the HCC database showed that DUSP9 was significantly highly expressed in tumor tissues compared to normal tissues, while SERPINE1 was lowly expressed, and there was no significant change in ENO2 and NTS (Figure 6A–D). At the same time, the protein expression profiles of the four characteristic genes downloaded from the HPA database showed the same results (Figure 6E–H).

Insulin Resistance and Immunity

IR is a chronic low-grade inflammatory condition.[26] The interaction between IR and inflammation initiates changes within the body's internal environment, significantly contributing to tumor development and disease progression. Under typical physiological conditions, chronic inflammation can activate immune cells to combat pathogens by producing reactive oxygen species (ROS). However, ROS may also disrupt insulin signaling by activating the mitogen-activated protein kinase (MAPK) family, thereby impairing insulin signal transmission and exacerbating insulin resistance. Additionally, oxidative damage caused by ROS is a significant factor in cellular mutations and increases the risk of tumor development. Moreover, IR might lead to higher blood glucose levels and more active fatty acid β-oxidation, perhaps worsening peroxidative damage and intensifying the inflammatory response, consequently forming a harmful feedback cycle.[27] An examination of liver cancer patients using the TIMER database showed differences in tumor infiltration levels related to somatic copy number changes for four genes (Supplementary Figure 2A–D); a correlation study between these four substances and immune cell groups indicated a remarkable connection with T follicular helper (TFH) cells, macrophages, and B cells (Supplementary Figure 2E–H), suggesting that immune cell activation caused by insulin resistance is a factor contributing to the less than ideal prognosis linked to TACE.

Validation of the Predicted Potency of the Signatures in the Cell Lines

To investigate TACE resistance mechanisms, we assessed the mRNA expression of DUSP9, ENO2, NTS, and SERPINE1 in five liver cancer cell lines. The analysis showed that the expression of the four characteristic genes in other liver cancer cells was significantly higher than that in normal cells. Among them, the expression of the four characteristic genes in the SNU-387 cell line was the highest, and the expression in the Hep3 B cell line was the lowest (Figure 7A–D). Therefore, we selected these two cell lines to analyze their sensitivity to TACE treatment. We analyzed the IC50 values of lobaplatin, a chemotherapeutic drug frequently used in TACE, under both normoxic and hypoxic conditions to simulate the TACE-induced environment. The results showed that the IC50 for Hep3B cells was 1.42 μg/mL under normoxia and 1.40 μg/mL under hypoxia (Figure 7E and F). For SNU-387 cells, the IC50 was 7.6 μg/mL under normoxia (Figure 7G) and 10.75 μg/mL under hypoxia (Figure 7H). The IC50 value of SNU-387 cells was higher than that of Hep3B cells under both normal oxygen and hypoxic conditions, and the IC50 value of SNU-387 further

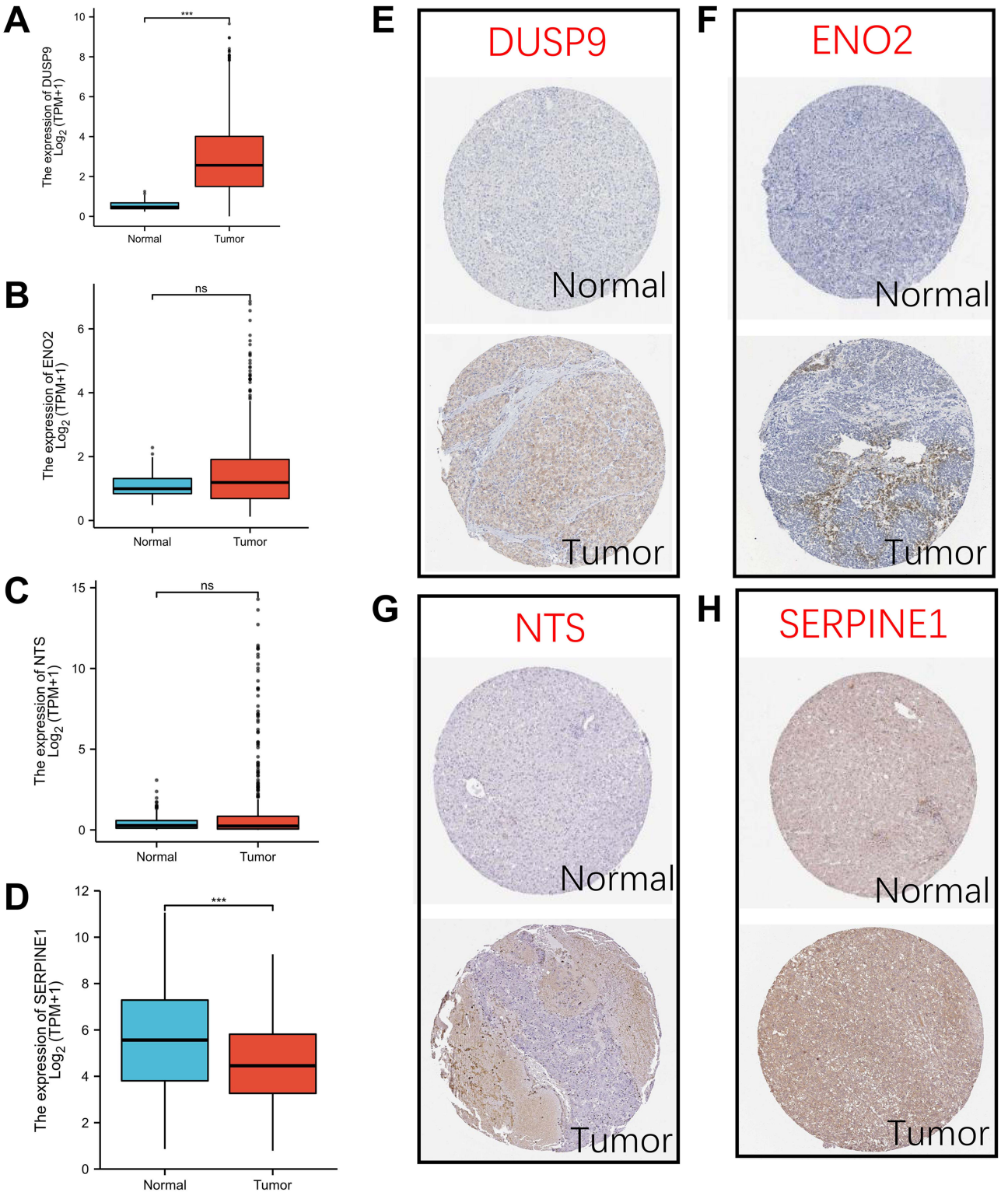

Figure 6 Validation of the expression of the four characteristic genes in the TCGA-LIHC database. (**A**–**D**) The box plot showed the expression differences of the four characteristic genes in normal and tumor tissues. (**E**–**H**) HPA (Human Protein Atlas) database was used to compare the expression of four characteristic genes in different tissues. ***P<0.001. ns, indicates no statistical significance.

Abbreviations: TCGA, The Cancer Genome Atlas; LIHC, Liver Hepatocellular Carcinoma; HPA, Human Protein Atlas.

https://doi.org/10.2147/JHC.S553710

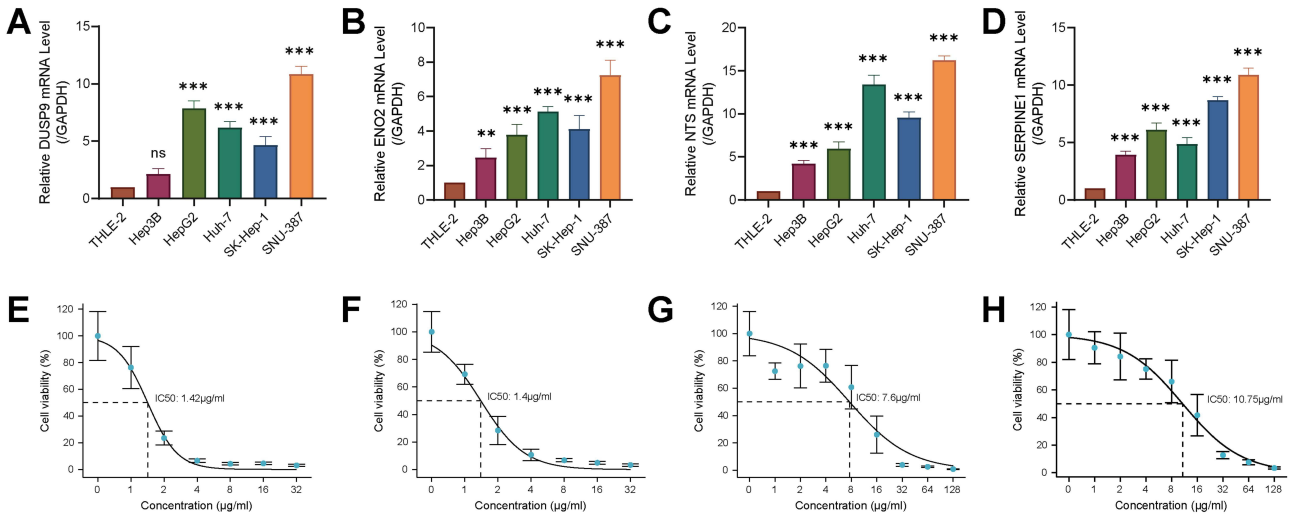

Figure 7 The selection of liver cancer cell lines and the WST-8 drug susceptibility test validated the validity of the prognostic features gene. (**A**–**D**) The mRNA expressions of the four molecules were detected in THLE-2 and five liver cancer cell lines using qRT-PCR. (**E** and **F**) IC50 of lobaplatin for Hep 3B detected in normoxic and hypoxic environments using WST-8. (**G** and **H**) The IC50 of lobaplatin in SNU-387 cells treated with lobaplatin in normoxic and hypoxic environments was determined by WST-8 method. **P<0.01, ***P<0.001.

Abbreviations: ns, indicates no statistical significance. qRT-PCR, Quantitative Real-Time Polymerase Chain Reaction.

increased under hypoxic conditions. This also indicated that SNU-387 is a TACE-resistant cell line. In short, the risk score we developed can effectively separate patients into those who respond to TACE and those who do not.

PD-98059 Can Be Used to Reverse Unresponsiveness to TACE

We analyzed differentially expressed genes (DEGs) between the high- and low-risk groups to address unresponsiveness to TACE. In the high-risk group, 15 genes exhibited significant upregulation, with a log2-fold change greater than 1.5 and a p-value less than 0.05. We inputted 22 genes into the CMap database to identify compounds that could counteract TACE resistance, focusing on those inducing opposite effects in the human hepatoma cell line SNU-387, which was used as a model for TACE non-responsiveness. We identified 87 chemicals with connectivity scores below −98, appearing in over 88 instances (Figure 8A). Notably, MEK inhibitors emerged as the most promising for overcoming TACE resistance, with MEK positioned immediately before the insulin signaling pathway (Figure 8B). Among these inhibitors, PD-98059 showed the greatest potential and accessibility, making it a potential candidate for reversing TACE resistance.

Molecular Docking

The average binding energies between PD-98059 and the target proteins DUSP9, ENO2, NTS, and SERPINE1 were −8.6 kcal/mol, −7.5 kcal/mol, −8.6 kcal/mol, and −6.9 kcal/mol, respectively. These negative values indicate spontaneous binding, and since all are below −5.0 kcal/mol, PD-98059 exhibits a strong affinity for each protein. The different interactions are depicted in the graph as follows: hydrophobic interactions with gray dotted lines, hydrogen bonds with blue solid lines, salt bridges with yellow dotted lines, parallel π-stacking interactions with grass-green dotted lines, and vertical π-stacking interactions with dark-green dotted lines. The analysis reveals that PD-98059 engages with the DUSP9 receptor protein through a hydrogen bond, two hydrophobic interactions, and a parallel π-stacking interaction. Specifically, it forms a hydrogen bond with the 329 PRO amino acid residue at 3.8 Å, hydrophobic interactions with the 313 LEU residue at 3.5 Å and 3.6 Å, and a parallel π-stacking interaction with the 317 TYR residue at 4.0 Å (Figure 9A–C).

The ligand PD-98059 interacts with the receptor protein ENO2 via three hydrogen bonds and four hydrophobic interactions. Specifically, it forms hydrogen bonds with 119 LYS, 378 THR, and 376 GLU amino acid residues at distances of 2.9, 3.1, and 3.9 Å, respectively. Additionally, it engages in hydrophobic interactions with ENO2 at distances of 3.8 Å, 3.9 Å, 3.6 Å, and 3.7 Å (Figure 9D–F). The ligand PD-98059 interacts with the receptor protein NTS through

https://doi.org/10.2147/JHC.S553710

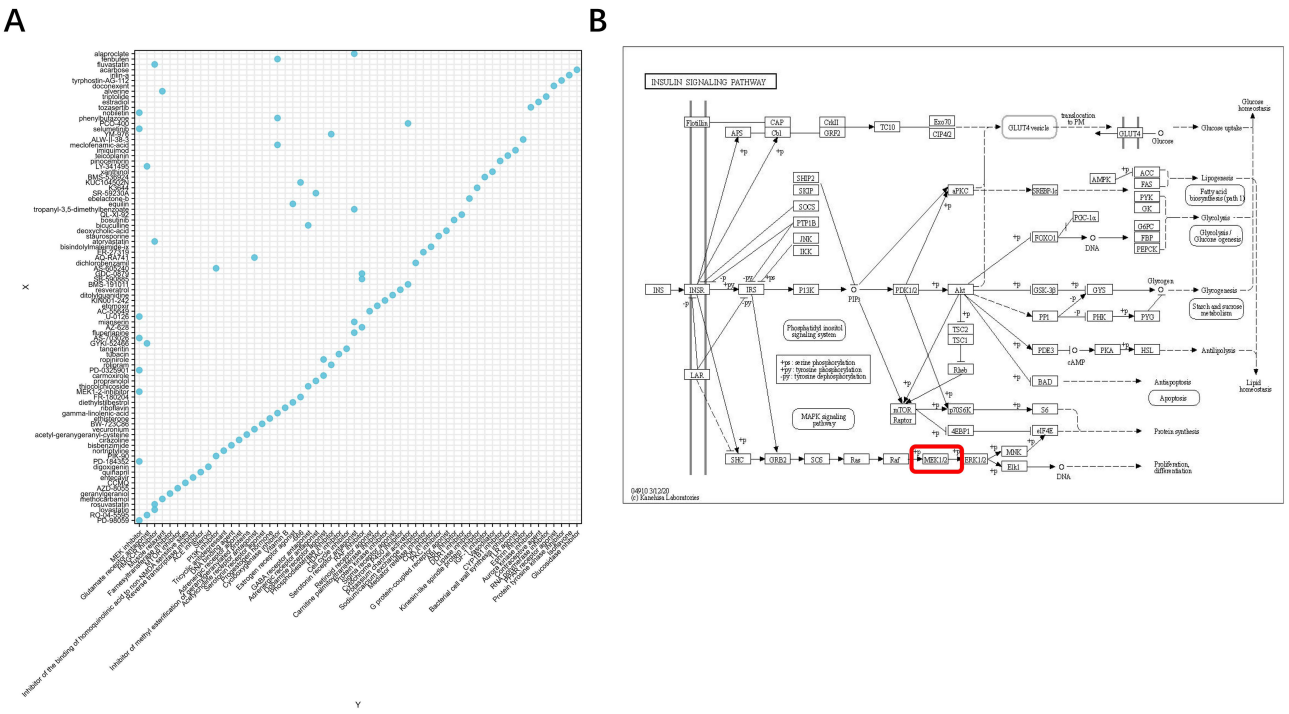

Figure 8 The MEK inhibitor PD-98059 was discovered as a potential drug to reverse TACE unresponsiveness. (**A**) Based on GSE14520-TACE subgroup, CMap was used to obtain compounds that can inhibit TACE resistance. The x-axis represents the class of the compound and the y-axis represents the name of the compound. (**B**) Schematic diagram of the insulin signaling pathway. Red circle, highlighting the position of the target gene MEK in the insulin signaling pathway.
Abbreviation: TACE, Transarterial chemoembolization.

various forces: a hydrogen bond with the 113 SER residue (3.1 Å), a vertical π-stacking force with the 116 PHE residue (5.1 Å), and hydrophobic forces with the 34 GLU, 110 ILE, 37 PHE, 115 ALA, and 54 TRP residues at distances of 3.6 Å, 3.7 Å, 4.0 Å, 3.5 Å, and 3.6 Å, respectively (Figure 9G–I). PD-98059, which is a ligand molecule, interacts with the SERPINE1 protein at the 213 PHE and 214 THR amino acid residues and forms two hydrogen bonds with a distance of 3.2 Å; moreover, it was involved in hydrophobic interactions with the 213 PHE, 258 LEU, and 253 ILE amino acid residues of SERPINE1, and the distances were 3.9 Å, 3.6 Å, and 3.8 Å respectively, and the ligand showed a parallel π - stacking interaction with the 213 PHE amino acid residue at a distance of 4.0 Å; meanwhile, a comparative study of two-dimensional force parameters corresponded to the results from three - dimensional structural analysis as illustrated in Figure 9J–L. The stability of the binding interaction between the ligand molecule PD-98059 and the four receptor proteins was ascribed to the aforementioned forces.

Validation of the Effect of PD-98059 on TACE Non-Response Cells

Following initial evaluation, the half-maximal inhibitory concentration (IC50) of PD-184352 for the SNU-387 cell line under hypoxic conditions was determined to be approximately 43.48 μg/mL, as illustrated in Figure 10A. Based on this concentration, we explored the sensitizing effect of PD-184352 on TACE. PD-184352, lobaplatin, or both, were added to SNU-387 cells and cultured under 1% hypoxia. One-way ANOVA revealed that lobaplatin ($P = 0.03$) and PD-184352 ($P < 0.0001$) significantly inhibited SNU-387 cell proliferation. Additionally, the combined use of PD-98059 and lobaplatin synergistically enhanced this inhibitory effect (Figure 10B).

Discussion

Liver cancer is a prevalent and aggressive digestive system tumor with poor prognosis.[28] Arterial embolism caused by TACE in the treatment of HCC and hypoxia caused by the inherent characteristics of the tumor can significantly promote the recurrence of TACE.[29] Insulin resistance, which is closely linked to hypoxia, also plays a role in promoting drug resistance in liver cancer cells.[30,31] However, the relationship between TACE and insulin resistance remains unclear.

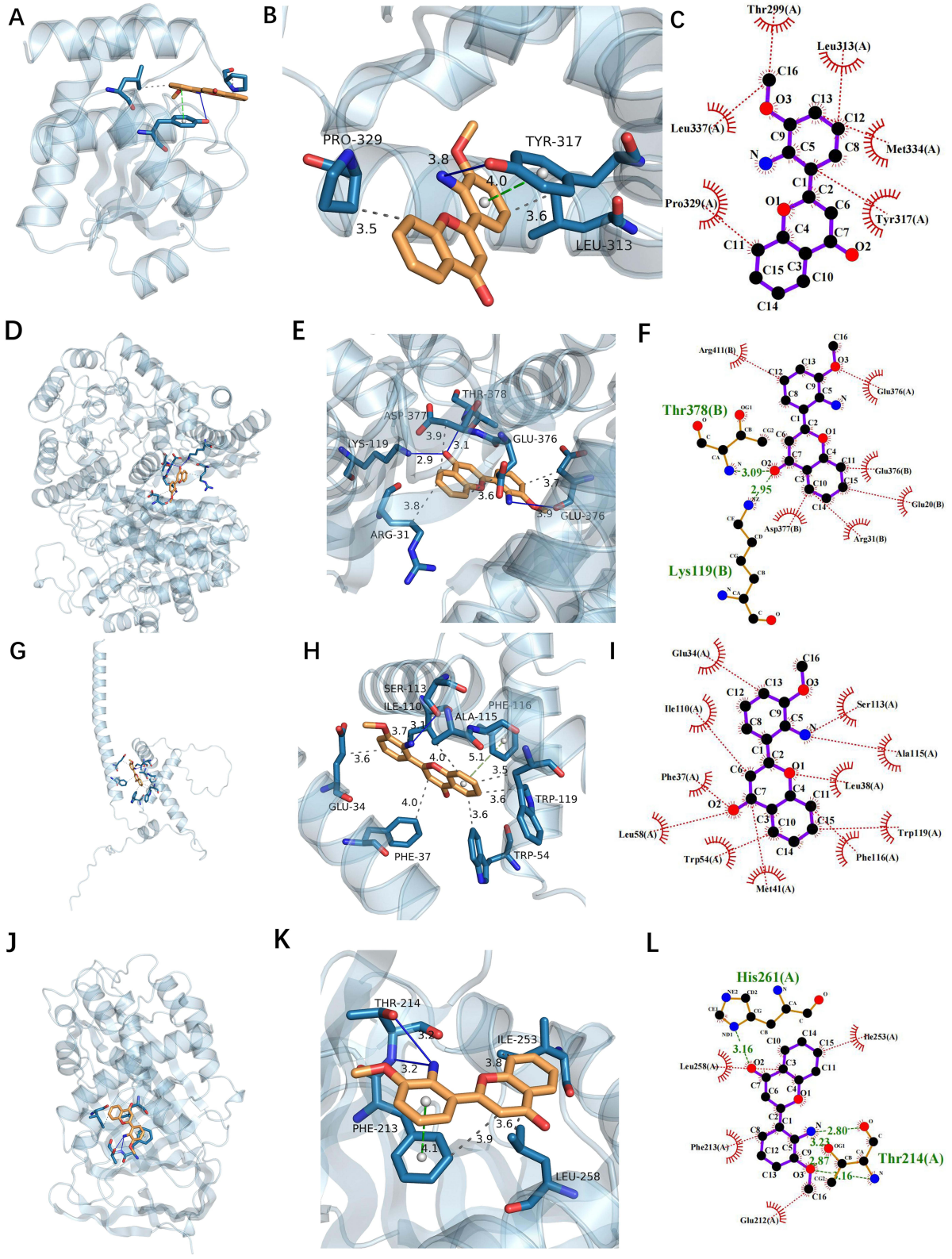

Figure 9 The Molecular docking. (**A**–**C**) DUSP9 and PD-98059. (**D**–**F**) ENO2 and PD-98059. (**G**–**I**) NTS and PD-98059. (**J**–**L**) SERPINE1 and PD-98059.

https://doi.org/10.2147/JHC.S553710

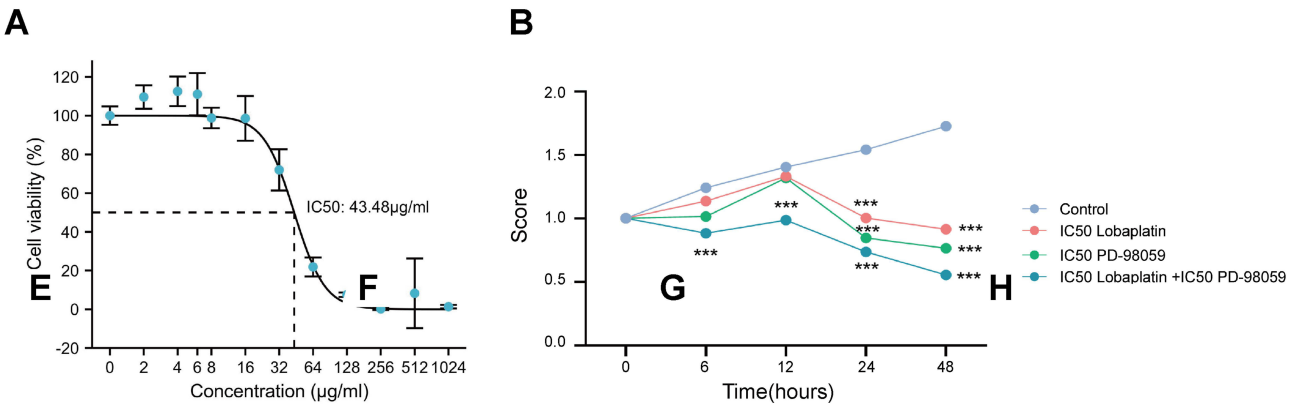

Figure 10 Validation of the effect of PD-98059 on TACE non-response cells. (**A**) The IC50 of PD-98059 in SNU-387 cells was detected by WST-8 method under hypoxic conditions. (**B**) Viability of SNU-387 cells treated with IC_{50} concentrations of lobaplatin, PD-98059, or their combination for graded time periods, as determined by the WST-8 assay. ***P<0.001.

Abbreviation: TACE, Transarterial chemoembolization.

Thus, the focus of this study was to construct diagnostic and prognostic models with good predictive performance for preoperative TACE resistance, and to try to explain the underlying mechanisms. A prognostic signature for insulin resistance in TACE treatment was developed using four genes identified from the expression patterns of DEGs between TACE-non-responders and responders and validated through cellular experiments. More importantly, the MEK inhibitor PD-98059 was selected as a drug that may reverse TACE non-responsiveness.

This study identified a significant enrichment of insulin resistance signaling pathways in TACE-non-responders compared to TACE-responders. Univariate Cox regression analysis identified 11 genes in GSE14520 that were associated to overall survival probability. The prognostic signature ultimately comprises four genes: DUSP9, ENO2, NTS, and SERPINE1. DUSP9, also known as MAP kinase phosphatase-4, belongs to the serine/threonine bispecific phosphatase family, and is significant in human pathology, including cardiac insufficiency, metabolic liver syndrome, diabetes, obesity, and cancer.[32] However, its involvement in TACE anergy remains unclear. Given the important role of DUSP9 in hypoxia, this warrants further investigation. ENO2, known to regulate islet function and promote the Warburg effect and cancer progression, was identified by Tang et al as one of the eight hypoxia-related genes predicting HCC prognosis, suggesting further investigation into its relationship with TACE.[33,34] Similarly, SERPINE1 or plasminogen activator inhibitor-1 (PAI-1) has been associated with poor cancer prognosis.[35,36] SERPINE1 is associated with poor prognosis in patients receiving TACE treatment, necessitating further research on the role of these genes, particularly their influence on TACE unresponsiveness.[18] Neurotensin (NTS), a 13-amino acid peptide found primarily in the enteroendocrine cells of the small intestine and released upon fat absorption, facilitates fatty acid translocation in the rat intestine and promotes the growth of various cancers. NTS signaling enhances tumor epithelial-mesenchymal transition (EMT) and invasiveness in liver cancer by activating the Wnt/β-catenin pathway.[37,38] However, its impact on the prognosis remains uncertain and warrants further investigation.

This study employed qRT-PCR was used to assess the mRNA expression levels of these four molecules in THLE-2 cells and five liver cancer cell lines. Then, the prognostic biomarkers we had set up were applied to classify SNU-387 as a TACE-non-responsive cell line and Hep3B as a TACE - responsive cell line; to imitate the therapeutic setting of TACE, lobaplatin treatment was combined with incubation at 1% oxygen tension; our results showed that Hep3B cells had more resistance to lobaplatin-induced cytotoxicity than SNU-387 cells whether under hypoxic or normal oxygen conditions, and it is worth noting that the half-maximal inhibitory concentration (IC50) for SNU-387 increased under hypoxic conditions when compared to normal oxygen conditions. Utilizing the L1000 gene expression analysis and the CMap build 1.0 database, we identified genes significantly activated in the GSE14520 high-risk group, MEK is located in the insulin signaling pathway, and PD-98059 became a potential candidate. At the same time, in view of its role of PD98059 as a specific and effective tool compound for MEK1/2 inhibition and its wide application in the study of the basic mechanism of cancer pathophysiology (such as liver cancer).[39,40] Its application in TACE treatment remains to be

explored, we preferred PD98059 in preliminary in vitro cell experiments. Our findings suggest that applying lobaplatin and PD98059 together under hypoxic conditions has a synergistic inhibitory effect on cell proliferation, indicating its potential as a new intraoperative or postoperative TACE therapeutic approach.

However, there are some limitations to our study. In the future, we will choose other clinical-grade MEK inhibitors (such as trimetinib and cobitinib) to conduct a comprehensive comparative evaluation of their efficacy and safety. Furthermore, future studies with predefined patient stratification and clinical endpoints are warranted to delineate the adjunctive benefits of PD-98059 to TACE and to generate solid clinical evidence. Finally, it is necessary to point out that using lobaplatin in our in vitro TACE model prevented us from evaluating any possible different effects when other chemotherapy agents are used along with MEK inhibition. Future research should focus on clarifying how MEK inhibitors work in the context of TACE and lay a theoretical basis for their clinical use. Future research should focus on technical standardization (eg, transition to qRT-PCR) and multicenter retrospective validation using archived tissues, such as paraffin-embedded tissue sections or archived serum samples in an independent, larger cohort of HCC patients receiving TACE treatment, to validate the robustness of our gene labeling to assess its universality. Subsequently, a prospective cohort study is critical to clearly determine its clinical utility, which may help stratify patients who are unlikely to benefit from TACE alone, thereby sparing them from ineffective treatment. In addition, the synergistic effect of PD-98059 (or a similar MEK inhibitor) combined with TACE was further evaluated in patient-derived organoids and humanized mouse PDX models. This lays the foundation for future biomarker-driven combination therapy trials, which also represents the ultimate transformation goal of this research route. Although we found insulin resistance-related genes associated with TACE resistance, we did not perform functional experiments under different glucose conditions to simulate the diabetic liver microenvironment. We acknowledge that this is a limitation, and future studies will include in vitro and in vivo models of hyperglycemia/insulin resistance to elucidate the underlying mechanisms of these findings.

Conclusion

In summary, we developed a four-gene signature based on insulin resistance that can mechanically predict TACE response in HCC, providing insights beyond the standard clinicopathological scores (eg, HAP, ART). Our model helps to stratify high-risk patients. In addition, preliminary in vitro studies have identified PD-98059 as a candidate sensitizer. We emphasize that these findings are fundamental and their clinical transformation requires further verification. While many genetic features have been proposed for HCC prediction, our study differs by focusing specifically on the IR pathway. This study provides a new perspective for predicting the prognosis and treatment of patients with HCC receiving TACE and is a new supplement to the prognosis of HCC. However, the clinical transformation of these studies remains uncertain, and the current public database lacks an independent cohort with TACE response + IR/glucose metabolism annotation. In the future, a prospective cohort study is required for further verification.

Data Sharing Statement

All the results are presented in the article. Further inquiries can be directed to the corresponding author of Weidong Wang.

Ethics Statement

The genomic and clinical data used in this study were obtained from publicly available databases (TCGA: https://portal.gdc.cancer.gov/; GEO: https://www.ncbi.nlm.nih.gov/geo/) and contain no personally identifiable information. According to Article 32 of the Measures for Ethical Review of Life Science and Medical Research Involving Human Subjects (National Health Commission of 340 China, effective February 18, 2023), this study was exempt from institutional ethics approval as it falls under the following categories: Use of publicly available, de-identified human data (Item 1). The study complies with the Declaration of Helsinki.

Funding

The research is supported by the Municipal Clinical Key Specialty-Interventional Radiology (Grant No. JRZDZK) and the "Geese Array Talent" Discipline Leader-2024 (Grant No. 2024-YZ-XKDTR-WWD-2024).

Disclosure

The authors report no conflicts of interest in this work.

References

1. Zhan Z, Chen B, Huang R, et al. Long-term trends and future projections of liver cancer burden in China from 1990 to 2030. *Sci Rep*. 2025;15(1):13120. doi:10.1038/s41598-025-96615-1
2. Bei H, Mai W, Chen W, Li M, Yang Y. Application of systemic treatment in conversion therapy options for liver cancer. *Front Oncol*. 2022;12:966821. doi:10.3389/fonc.2022.966821
3. Zeng ZM, Mo N, Zeng J, et al. Advances in postoperative adjuvant therapy for primary liver cancer. *World J Gastrointest Oncol*. 2022;14(9):1604–1621. doi:10.4251/wjgo.v14.i9.1604
4. Kim J, Kim JH, Ko E, et al. Model predicting survival in intermediate-stage HCC patients reclassified for TACE based on the 2022 BCLC criteria. *Cancers*. 2025;17(5). doi:10.3390/cancers17050894
5. Kudo M, Izumi N, Kokudo N, et al. Management of hepatocellular carcinoma in Japan: consensus-based clinical practice guidelines proposed by the Japan Society of Hepatology (JSH) 2010 updated version. *Dig Dis*. 2011;29(3):339–364. doi:10.1159/000327577
6. Yan J, Xie B, Tian Y, et al. iTRAQ-based proteome profiling of differentially expressed proteins in insulin-resistant human hepatocellular carcinoma. *Front Cell Develop Biol*. 2022;10:836041. doi:10.3389/fcell.2022.836041
7. Wei L, Li D, Chen H, et al. Elucidating the prognostic and therapeutic implications of insulin resistance genes in breast cancer: a machine learning-powered analysis. *Biology*. 2025;14(5):539. doi:10.3390/biology14050539
8. Mai Y, Meng L, Deng G, Qin Y. The role of type 2 diabetes mellitus-related risk factors and drugs in hepatocellular carcinoma. *J Hepatocell Carcinoma*. 2024;11:159–171. doi:10.2147/jhc.S441672
9. Caturano A, Erul E, Nilo R, et al. Insulin resistance and cancer: molecular links and clinical perspectives. *Mol Cell Biochem*. 2025;480(7):3995–4014. doi:10.1007/s11010-025-05245-8
10. Chen Z, Ding C, Chen K, Gu Y, Qiu X, Li Q. Investigating the causal association between obesity and risk of hepatocellular carcinoma and underlying mechanisms. *Sci Rep*. 2024;14(1):15717. doi:10.1038/s41598-024-66414-1
11. Liu G, Xia F, Fan G, et al. Type 2 diabetes mellitus worsens the prognosis of intermediate-stage hepatocellular carcinoma after transarterial chemoembolization. *Diabetes Res Clin Pract*. 2020;169:108375. doi:10.1016/j.diabres.2020.108375
12. Tan Y, Xuan N, Guo R, et al. Characteristics, diagnosis, treatment and prognosis of double primary hepatic cancer: experience based on a series of 12 cases. *Am J Transl Res*. 2024;16(8):4234–4245. doi:10.62347/piwa3282
13. Jia KF, Wang H, Yu CL, et al. ASARA, a prediction model based on Child-Pugh class in hepatocellular carcinoma patients undergoing transarterial chemoembolization. *Hepatobiliary Pancreatic Dis Int*. 2023;22(5):490–497. doi:10.1016/j.hbpd.2022.02.007
14. Jia K, Yin W, Gao Z, et al. Recommendation of mHAP and ABCR scoring systems for the decision-making of the first and subsequent TACE session in HCC patients. *Eur J Gastroenterol Hepatol*. 2023;35(4):461–470. doi:10.1097/meg.0000000000002515
15. Shen L, Jiang Y, Lu L, et al. Dynamic prognostication and treatment planning for hepatocellular carcinoma: a machine learning-enhanced survival study using multi-centric data. *Innov Med*. 2025;3(2):100125. doi:10.59717/j.xinn-med.2025.100125
16. Feng G, Xu H, Wan S, et al. Twelve practical recommendations for developing and applying clinical predictive models. *Innovat Med*. 2024;2(4):100105. doi:10.59717/j.xinn-med.2024.100105
17. Zhang C, Hu Q, Meng H, et al. Integrative multi-omics and functional validation reveal the role of the tace refractoriness-associated gene ATP1B3 in hepatocellular carcinoma. *J Hepatocell Carcinoma*. 2025;12:2565–2583. doi:10.2147/jhc.S537990
18. Xia Z, Zhao W, Liu J, et al. A three-gene signature for predicting the prognosis of patients treated with transarterial chemoembolization (TACE) and identification of PD-184352 as a potential drug to reverse nonresponse to TACE. *J Oncol*. 2022;2022:2704862. doi:10.1155/2022/2704862
19. Subramanian A, Narayan R, Corsello SM, et al. A next generation connectivity map: L1000 platform and the first 1,000,000 profiles. *Cell*. 2017;171(6):1437–1452.e17. doi:10.1016/j.cell.2017.10.049
20. Yang J, Sun Y, Xu F, et al. Autophagy and glycolysis independently attenuate silibinin-induced apoptosis in human hepatocarcinoma HepG2 and Hep3B cells. *Hum Exp Toxicol*. 2021;40(12):2048–2062. doi:10.1177/09603271211017609
21. Pozo Garcia V, Çobanoğlu TS, Hammer HS, et al. Nutrient environment improves drug metabolic activity in human iPSC-derived hepatocytes and HepG2. *Arch Toxicol*. 2025;99(11):4493–4511. doi:10.1007/s00204-025-04139-4
22. Han J, Jang KL. All-trans retinoic acid downregulates HBx levels via E6-associated protein-mediated proteasomal degradation to suppress hepatitis B virus replication. *PLoS One*. 2024;19(6):e0305350. doi:10.1371/journal.pone.0305350
23. Tarekegn LH, Shuster SO, Davis CM. Insulin-resistant Huh-7 cells as a model for nonalcoholic fatty liver disease. *Biophys J*. 2024;123(3):411a. doi:10.1016/j.bpj.2023.11.2515
24. Chang Z, Karmakar B, Lu H, et al. Preparation of gelatin/Ag NPs under ultrasound condition: a potent and green bio-nanocomposite for the treatment of pleomorphic hepatocellular carcinoma, morris hepatoma, and novikoff hepatoma. *Arabian J Chem*. 2022;15(6):103858. doi:10.1016/j.arabjc.2022.103858
25. Zhao Z, Su J, Zhao J, et al. Curcumin inhibits invasion and metastasis of human hepatoma cells through Bclaf1-mediated Wnt/β-catenin signalling. *Food Agric Immunol*. 2022;33(1):664–676. doi:10.1080/09540105.2022.2113864
26. Klimczak S, Śliwińska A. Epigenetic regulation of inflammation in insulin resistance. *Semin Cell Dev Biol*. 2024;154(Pt C):185–192. doi:10.1016/j.semcdb.2022.09.004
27. Ayer A, Fazakerley DJ, James DE, Stocker R. The role of mitochondrial reactive oxygen species in insulin resistance. *Free Radic Biol Med*. 2022;179:339–362. doi:10.1016/j.freeradbiomed.2021.11.007
28. Novikova MV, Khromova NV, Kopnin PB. Components of the hepatocellular carcinoma microenvironment and their role in tumor progression. *Biochem Biokhimiia*. 2017;82(8):861–873. doi:10.1134/s0006297917080016
29. Zong S, Huang G, Pan B, Zhao S, Ling C, Cheng B. A hypoxia-related miRNA-mRNA signature for predicting the response and prognosis of transcatheter arterial chemoembolization in hepatocellular carcinoma. *J Hepatocell Carcinoma*. 2024;11:525–542. doi:10.2147/jhc.S454698

30. Xia QS, Wu F, Wu WB, et al. Berberine reduces hepatic ceramide levels to improve insulin resistance in HFD-fed mice by inhibiting HIF-2α. *Biomed Pharmacother*. 2022;150:112955. doi:10.1016/j.biopha.2022.112955
31. Nwabo Kamdje AH, Seke Etet PF, Kipanyula MJ, et al. Insulin-like growth factor-1 signaling in the tumor microenvironment: carcinogenesis, cancer drug resistance, and therapeutic potential. *Front Endocrinol*. 2022;13:927390. doi:10.3389/fendo.2022.927390
32. Wang J, Wei T, Zhang W, et al. Inhibition of miR-194-5p avoids DUSP9 downregulation thus limiting sepsis-induced cardiomyopathy. *Sci Rep*. 2024;14(1):20313. doi:10.1038/s41598-024-71166-z
33. Tang Y, Zhang H, Chen L, Zhang T, Xu N, Huang Z. Identification of hypoxia-related prognostic signature and competing endogenous RNA regulatory axes in hepatocellular carcinoma. *Int J Mol Sci*. 2022;23(21):13590. doi:10.3390/ijms232113590
34. Jiang X, Chen Z, Zhu J, et al. E2F1 promotes Warburg effect and cancer progression via upregulating ENO2 expression in Ewing sarcoma. *Mol Med Rep*. 2022;26(1). doi:10.3892/mmr.2022.12753
35. Lv J, Yu C, Tian H, Li T, Yu C. Expression of Serpin Family E Member 1 (SERPINE1) is associated with poor prognosis of gastric adenocarcinoma. *Biomedicines*. 2023;11(12):3346. doi:10.3390/biomedicines11123346
36. Zhu C, Liu H, Li Z, et al. Prognostic significance and therapeutic potential of SERPINE1 in head and neck squamous cell carcinoma. *Cancer Med*. 2025;14(2):e70605. doi:10.1002/cam4.70605
37. Xiao P, Long X, Zhang L, et al. Neurotensin/IL-8 pathway orchestrates local inflammatory response and tumor invasion by inducing M2 polarization of tumor-associated macrophages and epithelial-mesenchymal transition of hepatocellular carcinoma cells. *Oncoimmunology*. 2018;7(7):e1440166. doi:10.1080/2162402x.2018.1440166
38. Mazella J. Deciphering mechanisms of action of sortilin/neurotensin receptor-3 in the proliferation regulation of colorectal and other cancers. *Int J Mol Sci*. 2022;23(19):11888. doi:10.3390/ijms231911888
39. Chen YF, Yang YN, Chu HR, et al. Role of integrin αvβ3 in doxycycline-induced anti-proliferation in breast cancer cells. *Front Cell Develop Biol*. 2022;10:829788. doi:10.3389/fcell.2022.829788
40. Liu Y, Sui A, Sun J, Wu Y, Liu F, Yang Y. c-Jun-mediated JMJD6 restoration enhances resistance of liver cancer to radiotherapy through the IL-4-activated ERK pathway. *Cell Biol Int*. 2023;47(8):1392–1405. doi:10.1002/cbin.12026